

S. Paganelli¹ · M. Łącki² · V. Ahufinger³ · J. Zakrzewski^{2,4} ·
 A. Sanpera^{5,1}

Spin effects in Bose-Glass phases

May 27, 2022

Keywords Ultracold atoms, Bose glass, Spin-1 Bose Hubbard model

Abstract We study the mechanism of formation of Bose glass (BG) phases in the spin-1 Bose Hubbard model when diagonal disorder is introduced. To this aim, we analyze first the phase diagram in the zero-hopping limit, there disorder induces superposition between Mott insulator (MI) phases with different filling numbers. Then BG appears as a compressible but still insulating phase. The phase diagram for finite hopping is also calculated with the Gutzwiller approximation. The bosons' spin degree of freedom introduces another scattering channel in the two-body interaction modifying the stability of MI regions with respect to the action of disorder. This leads to some peculiar phenomena such as the creation of BG of singlets, for very strong spin correlation, or the disappearance of BG phase in some particular cases where fluctuations are not able to mix different MI regions.

PACS numbers: 03.75.Mn, 64.60.Cn, 67.85.-d

1 Introduction

Ultracold atomic gases can be described by interacting atoms with an internal spin, corresponding to a low-energy hyperfine level F . If the spin orientation is fixed by an external magnetic field, as it happens when the gas is confined in magnetic trap, a scalar model is sufficient to describe the system. Conversely, if the spin orientation is not externally constrained, as in the case of optical trapping, the spinor character of the gas has to be taken into account. For bosons trapped in a deep optical lattice potential the system is well described by the spinor Bose-Hubbard (BH) model [1]. Bosonic interactions, treated as two-body contact collisions, are sensitive to the spin degree of freedom and contribute to the orderings at zero temperature.

As in the scalar case [2], the competition between hopping and interactions leads to a quantum phase transition between spinor superfluid (SF) condensate and a Mott insulator (MI) state [1, 3, 4]. Spin correlation introduces magnetic ordering which contribute to the stability of one phase with respect to the other. Moreover, the presence of spin scattering channels influences also the stability of the MI phases in the presence of different types of disorder.

Disorder plays an essential role in condensed matter physics and it has been shown to be an essential ingredient for studies of conductivity, transport, high-Tc superconductivity, neural networks or quantum chaos to mention few examples (see the review[5] and references therein). Disorder can be produced in ultracold

1: Grup de Física Teòrica: Informació i Fenòmens Quàntics, Universitat Autònoma de Barcelona, 08193 Bellaterra, Spain
 E-mail: paganelli@ifae.es

2: Instytut Fizyki imienia Mariana Smoluchowskiego, Uniwersytet Jagielloński,
 ulica Reymonta 4, 30-059 Kraków, Poland

3: Grup d'Òptica: Departament de Física Universitat Autònoma de Barcelona,
 08193 Bellaterra, Spain

4: Mark Kac Complex Systems Research Center, Jagiellonian University, Kraków, Poland

5: ICREA-Institució Catalana de Recerca i Estudis Avançats,
 Lluís Companys 23, 08010 Barcelona, Spain

atoms in a *controlled* and *reproducible* way. Standard methods to achieve such a controlled disorder are the use of speckle patterns [6, 7] which can be added to the confining potential, or optical superlattices created by the simultaneous presence of optical lattices of incommensurate frequencies [8, 9, 10]. Other methods include using an admixture of different atomic species randomly trapped in sites distributed across the sample and acting as impurities [11, 12], or the use of inhomogeneous magnetic fields which modify randomly, close to a Feshbach resonance, the scattering length of atoms in the sample depending on their spatial position [13, 14].

Recently, the phase diagram of the spin-1 BH model in two dimensions (2D) in the presence of disorder has been studied with a Gutzwiller mean field approximation [15]. As in the scalar case [2], a gapless Bose-glass (BG) insulator phase appears, characterised by finite compressibility and exponentially decaying superfluid correlations in space, but, because of the spin interaction, the phase diagram changes considerably.

In this paper we focus on the spin-1 BH model in the presence of diagonal disorder and analyse the role of spin correlations in the formation of the BG phase. We study in detail the zero-hopping limit (atomic case). We provide, in this simple case, the phase diagram corresponding to different types of disorder and show how spin correlations can prevent the formation of the BG between some MI regions. This fully analytical approach allows to easily visualise the mechanism of formation of the BG in terms of superpositions between MI phases with different filling factors. We also provide, in some cases, the complete phase diagram for finite tunnelling using a numerical mean field Gutzwiller approximation. In particular, we show the case of large spin interactions where a BG of singlets emerges. We analyse the case in which the disorder is directly introduced in the two-body scattering lengths, associated with total spin of scattering particles $s = 0$ and $s = 2$, instead of in the Hamiltonian parameters directly. This represents a more realistic scenario since small fluctuations in the scattering lengths can be introduced by optical Feshbach resonances. We observe the absence of BG phase for ferromagnetic spin interactions and disorder in the $s = 2$ scattering length, confirming that, in this limit, the spinor model is equivalent to the scalar case.

The paper is organised as follows: in Sec. 2 we introduce the BH model. Then we proceed to compare the effect of diagonal disorder in the local potential or in the interaction. In particular, we compare the cases in which disorder is in the local parameters of the Hamiltonian (Sec. 3) with the case in which disorder is introduced directly in the two-body scattering lengths corresponding to the collision channel with total spin $s = 0$ and $s = 2$ (Sec. 4). Finally, in Sec. 5 we present our conclusions.

2 Model

Low energy spin-1 bosons loaded in optical lattices, sufficiently deep so that only the lowest energy band is relevant, can be described by the spinor BH model. The corresponding Hamiltonian is [1]:

$$\hat{H} = -t \sum_{\langle i,j \rangle, \sigma} \hat{a}_{i\sigma}^\dagger \hat{a}_{j\sigma} + \sum_i \left[\frac{U_0}{2} \hat{n}_i (\hat{n}_i - 1) + \frac{U_2}{2} (\hat{\mathbf{S}}_i^2 - 2\hat{n}_i) - \mu \hat{n}_i \right], \quad (1)$$

where $\langle i, j \rangle$ indicates that the sum is restricted to nearest neighbours in the lattice and $\hat{a}_{i\sigma}^\dagger$ ($\hat{a}_{i\sigma}$) denotes the creation (annihilation) operator of a boson in the lowest Bloch band localised on site i with spin component $\sigma = 0, \pm 1$.

The first term in (1) represents the kinetic energy and describes spin independent hopping between nearest-neighbour sites with tunnelling amplitude t . The second and third term account for spin independent and spin dependent on site interactions, respectively. These energies at site i are defined as $U_{0,2} = c_{0,2} \int d\mathbf{r} w^4(\mathbf{r} - \mathbf{r}_i)$ with $c_0 = 4\pi\hbar^2(a_0 + 2a_2)/(3m)$ and $c_2 = 4\pi\hbar^2(a_2 - a_0)/(3m)$, where a_S with $S = 0, 2$ is the s -wave scattering length corresponding to the channel with total spin S [16, 17] and $w(\mathbf{r} - \mathbf{r}_i)$ is the Wannier function of the lowest band at site i . While the second term of (1) is spin independent and equivalent to the interaction energy for scalar bosons, the third term represents the energy associated with spin configurations within lattice sites with

$$\hat{\mathbf{S}}_i = \sum_{\sigma\sigma'=0,\pm 1} \hat{a}_{\sigma i}^\dagger \mathbf{F}_{\sigma\sigma'} \hat{a}_{\sigma' i}, \quad (2)$$

being the spin operator at site i and \mathbf{F} the traceless spin-1 matrices. $\hat{\mathbf{S}}_i$'s components obey standard angular momentum commutation relations $[\hat{S}_i, \hat{S}_j] = i\epsilon_{ijk}\hat{S}_k$. The spin-interaction term favours a configuration with total magnetisation zero for $U_2 > 0$, denoted as polar and sometimes antiferromagnetic. The ferromagnetic configuration where spins add to a maximal possible value corresponds to $U_2 < 0$ [16, 17, 18]. In the grand

canonical approach the total number of particles is controlled by the last term of (1) where μ is the chemical potential and

$$\hat{n}_i = \sum_{\sigma=0,\pm 1} \hat{n}_{i,\sigma}, \quad (3)$$

is the total number of bosons on site i . Hamiltonian (1) can be straightforwardly derived from the microscopical description of bosonic atoms, with a hyperfine spin $F = 1$, loaded in a deep optical lattice and considering the two-body short range (s-wave) collisions. More details about the derivation can be found in [3, 16, 17, 19, 20].

Notice also that, since the orbital part of the wave function in one lattice site is the product of Wannier functions for all the atoms, it is symmetric under permutation of any two atoms. Therefore, the spin part of the wavefunction should also be symmetric due to Bose statistics. This imposes $s_i + n_i$ to be even [21], being s_i and n_i the quantum numbers labelling the eigenvalues of $\hat{\mathbf{S}}_i$ and \hat{n}_i , respectively. In alkaline atoms usually, the scattering lengths are similar, $a_0 \simeq a_2$, and the symmetry of the Hamiltonian becomes SU(3) instead of SU(2). That implies $|U_0| \gg |U_2|$.

As in the scalar case, the spinor BH system exhibits a quantum phase transition between superfluid and insulating states [1, 3]. In the insulating states, fluctuations in the atom number per site are suppressed and virtual tunnelling gives rise to effective spin exchange interactions that determine a rich phase diagram in which different insulating phases differ by their spin correlations.

2.1 Atomic limit ($t = 0$)

Hamiltonian (1) becomes diagonal in the limit of vanishing hopping. In this limit it reduces to the sum of local terms $\hat{H} \rightarrow \sum_i \hat{H}_{0,i}$ with

$$\hat{H}_0 = \frac{U_0}{2} \hat{n}(\hat{n} - 1) + \frac{U_2}{2} (\hat{\mathbf{S}}^2 - 2\hat{n}) - \mu \hat{n}, \quad (4)$$

(site indexes are omitted if the system is homogeneous). Eigenstates of \hat{H}_0 are denoted with $|n, s, m\rangle$, where the quantum numbers refer to the three commuting local observables

$$\begin{aligned} \hat{n} |n, s, m\rangle &= n |n, s, m\rangle, \\ \hat{\mathbf{S}}^2 |n, s, m\rangle &= s(s+1) |n, s, m\rangle, \\ \hat{S}_z |n, s, m\rangle &= m |n, s, m\rangle, \end{aligned}$$

with energies $H_0 |n, s, m\rangle = E_0(n, s) |n, s, m\rangle$ given by

$$E_0(n, s) = -\mu n + \frac{U_0}{2} n(n-1) + \frac{U_2}{2} (s(s+1) - 2n). \quad (5)$$

From Eq.(5), one can easily deduce the structure of the ground state of the insulator phases in the limit $t = 0$. In the atomic limit without disorder, only MI phases exist. SF corresponds to the points separating MI intervals with different fillings (as can be inferred from $t \rightarrow 0$ limit). This means that, at fixed μ , the ground state has an integer filling n . The boundaries corresponding to the degeneracy points between two fillings n_1 and n_2 satisfy the condition $E_0(n_1, s_1) = E_0(n_2, s_2)$. Any MI region with filling n and fixed U_2 is defined for $\mu_-(n) < \mu < \mu_+(n)$, where $\mu_{\pm}(n)$ are the boundaries of the region.

For antiferromagnetic interactions, $U_2 > 0$, the minimum energy E_0^{min} is attained with minimum s , its specific value depending of the number of atoms per site. Thus, for the even filling factor, the minimum spin is zero and the state is described as $|0, 0, n\rangle$ with n even. This state is known as spin singlet insulator [22]. If the atom number per site is odd, then the minimum spin per site is one and the state reads $|1, m, n\rangle$ in the absence of disorder.

Let us calculate explicitly μ_{\pm} . For $U_2 > 0$ (antiferromagnetic case) we must distinguish between odd and even occupation lobes:

(1) n odd: the boundaries $\mu_{\pm}(n)$ are obtained by imposing $E_0(n, 1) = E_0(n \pm 1, 0)$

$$\begin{aligned} \mu_- &= (n-1)U_0, \\ \mu_+ &= nU_0 - 2U_2. \end{aligned} \quad (6)$$

Odd lobes exist only for $\mu_- < \mu_+$ that is, for $U_2/U_0 < 0.5$.

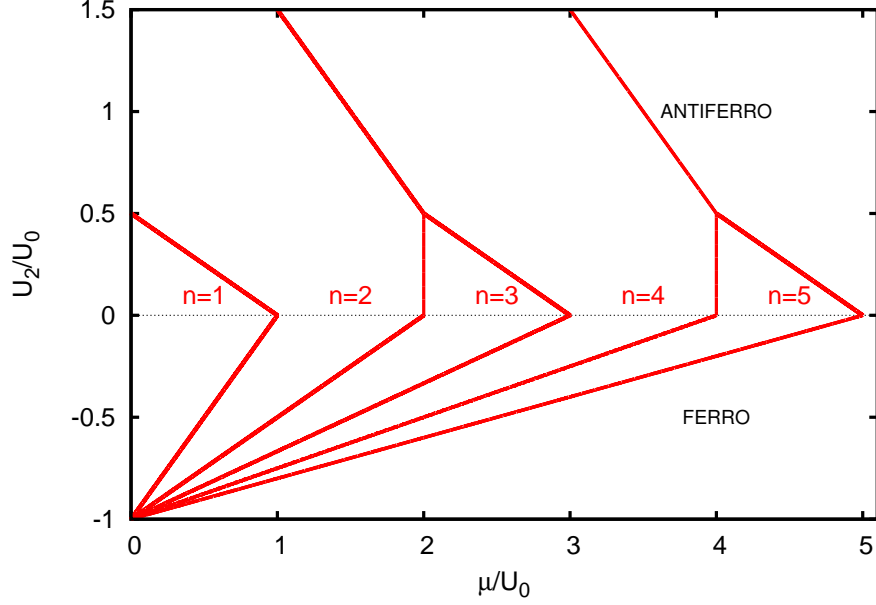


Fig. 1 Phase diagram of the spinor $F = 1$ BH model in the limit $t = 0$. Each region corresponds to a MI phase with a different occupation number. For $U_2/U_0 > 0$ the system has zero magnetization (antiferro) and for $U_2/U_0 < 0$ the system is in a ferromagnetic phase

(2) n even: for $U_2/U_0 < 0.5$, $\mu_{\pm}(n)$ are obtained by imposing $E_0(n, 0) = E_0(n \pm 1, 1)$

$$\begin{aligned}\mu_- &= (n-1)U_0 - 2U_2, \\ \mu_+ &= nU_0,\end{aligned}\tag{7}$$

while, for $U_2/U_0 > 0.5$ the condition $E_0(0, n) = E_0(0, n \mp 2)$ leads to

$$\begin{aligned}\mu_- &= \left(n - \frac{1}{2}\right)U_0 - U_2, \\ \mu_+ &= \left(n + \frac{1}{2}\right)U_0 - U_2,\end{aligned}\tag{8}$$

For $U_2 < 0$ (ferromagnetic case) the maximum value of the spin is given by $s = n$ and the condition for the boundaries $E_0(n, n) = E_0(n \mp 1, n)$ reads

$$\begin{aligned}\mu_- &= (n-1)(U_0 + U_2), \\ \mu_+ &= n(U_0 + U_2).\end{aligned}\tag{9}$$

The atomic-limit phase diagram is depicted in Fig. 1, the MI intervals obtained fixing U_2 correspond to the basis of the MI lobes in the $t/U_0 - \mu/U_0$ plane[15]. In the antiferromagnetic region, one can see that the formation of singlet stabilises the even MI lobes while the odd lobes shrink. For $U_2 < 0$, U_2 , eq. (1) reduces to the scalar Hamiltonian with $U_0 + U_2$ put in place of U_0 . Notice that for $U_2 < -U_0$ the spectrum (5) is not bounded from below and the model becomes unstable.

3 Diagonal disorder in the Hamiltonian's parameters

Starting from this scenario, we proceed to analyse the stability of the MI phase in the presence of disorder. We start by analysing local fluctuations ε_i added either to the homogeneous chemical potential μ , or on the interaction potential U_0 or U_2 . We consider ε_i to be a random variable defined for every site i with a

given probability distribution $p(\varepsilon)$. Here we consider a bounded probability distribution that is $-\Delta < \varepsilon_i < \Delta$. Disorder mixes together different MI regions so that degeneracy between different fillings appears. So, between MI intervals, regions can appear where filling is not defined and correspondingly a BG phase appears. Being the probability distribution bounded, the BG phase appears only around the original boundaries and its extension depends on Δ . On the other hand, deep inside the MI, small fluctuations of the disordered parameter are not able to mix different fillings and the state remains stable in the corresponding MI phase.

The first case we study is the disorder in the chemical potential. This type of disorder can be produced introducing some random inhomogeneities in the local potential $\mu_j = \mu + \varepsilon_j$. Fixing U_2 , disorder in μ_j corresponds to horizontal fluctuations of maximum amplitude Δ in the atomic-limit phase diagram. The new boundaries for the MI phases are given by replacing $\mu_{\pm} \rightarrow \mu_{\pm} \mp \Delta$ as can be observed in the top panel of Fig. 2. We notice that BG regions always appear between MI lobes with width (in μ) of the order of 2Δ . Since odd lobes shrunk by U_2 , they are more unstable and disorder can make them disappear.

When $U_2/U_0 > 0.5$ disorder mixes together only even occupations so BG is formed by singlets [15]. The finite-hopping phase diagram for this case is displayed in the bottom panel of Fig. 2, where we have used the condensate fraction [8] as an order parameter to separate SF from BG phase. Our calculations are done within the mean field Gutzwiller approach, which is able to take into account inhomogeneities caused by disorder [15]. The MI phase is characterised by vanishing fluctuations in the density (or zero compressibility) while the BG corresponds to finite density fluctuations and zero condensate fraction. In this plot one can see the disappearance of the odd occupation MI lobes. Numerical calculation shows that $\langle \mathbf{S}^2 \rangle = 0$ meaning that also the BG phase is formed by singlets [15]. Note that, even if we found it adding disorder in the chemical potential, singlet BG appears also for disorder in U_0 and U_2 , the only necessary condition being $U_2/U_0 > 0$.

Disorder in U_2 corresponds to fluctuations along the vertical direction of the phase diagram in Fig. 1. The resulting phase diagram in the atomic limit is shown in the top panel of Fig. 3. The new boundaries are obtained changing μ_{\pm} in Eqs. (6-9) replacing $U_2 \rightarrow U_2 \mp \Delta$ for $U_2/U_0 < 0$, and $U_2 \rightarrow U_2 \pm \Delta$ for $U_2/U_0 > 0$. One consequence is that, for $U_2/U_0 < 0.5$ no BG appears between even and odd lobes with higher occupation (that is between lobes with occupation $n = 2m$ and $n = 2m + 1$) where the boundaries are vertical. This is true for $|U_2| > \Delta$ otherwise disorder can mix together ferromagnetic and antiferromagnetic regions, and BG appears between all the lobes. Note that, in the antiferromagnetic limit, the shrinking of the MI lobes is almost independent on the occupation and depends only on U_2 . In the ferromagnetic case, the MI lobes become more unstable increasing n disappearing for $n > (U_0 + U_2 + \Delta)/(2\Delta)$.

So far we have analysed the effects of fluctuations along vertical and horizontal directions in the phase plane. More generally, a diagonal disorder can be interpreted in terms of fluctuations of a certain amplitude $\tilde{\Delta}$ along some direction, possibly depending on the position (μ^0, U_2^0) in the atomic phase diagram, in which is centred. Let us denote the direction as a straight line

$$\frac{U_2}{U_0} = a \frac{\mu}{U_0} + b, \quad (10)$$

In general, if a MI boundary lies along the direction of fluctuations defined by a specific type of disorder, no BG would appear for sufficiently small disorder strength.

In the case of disorder in U_0 , the fluctuations occur along the direction defined by the parameters in (10) $a = U_2^0/\mu^0$ and $b = 0$ with amplitude $\tilde{\Delta} = 2\Delta \sqrt{(\mu^0)^2 + (U_2^0)^2}/(U_0 - \Delta^2)$. The new boundaries are obtained modifying μ_{\pm} by the replacements $U_0 \rightarrow U_0 \mp \Delta$. This causes a progressive shrinking of all the lobes which disappear for high densities. It is worth noting that odd lobes disappear independently on U_2 for $n > \frac{U_0 + \Delta}{2\Delta}$. The resulting atomic phase diagram is shown in the bottom panel of Fig. 3.

4 Disorder in the scattering lengths

As pointed out in Sec. 2, U_0 and U_2 depend on the scattering lengths a_0 and a_2 via the relations

$$\begin{aligned} U_0 &= \alpha_0 + 2\alpha_2, \\ U_2 &= \alpha_0 - \alpha_2, \end{aligned} \quad (11)$$

having introduced the renormalized parameters $\alpha_s = a_s 4\pi \int d\mathbf{r} w^4(\mathbf{r} - \mathbf{r}_i)/(3m)$. Both α_0 and α_2 can fluctuate locally in the presence of optical Feshbach resonances, so disorder can be introduced in these variables and

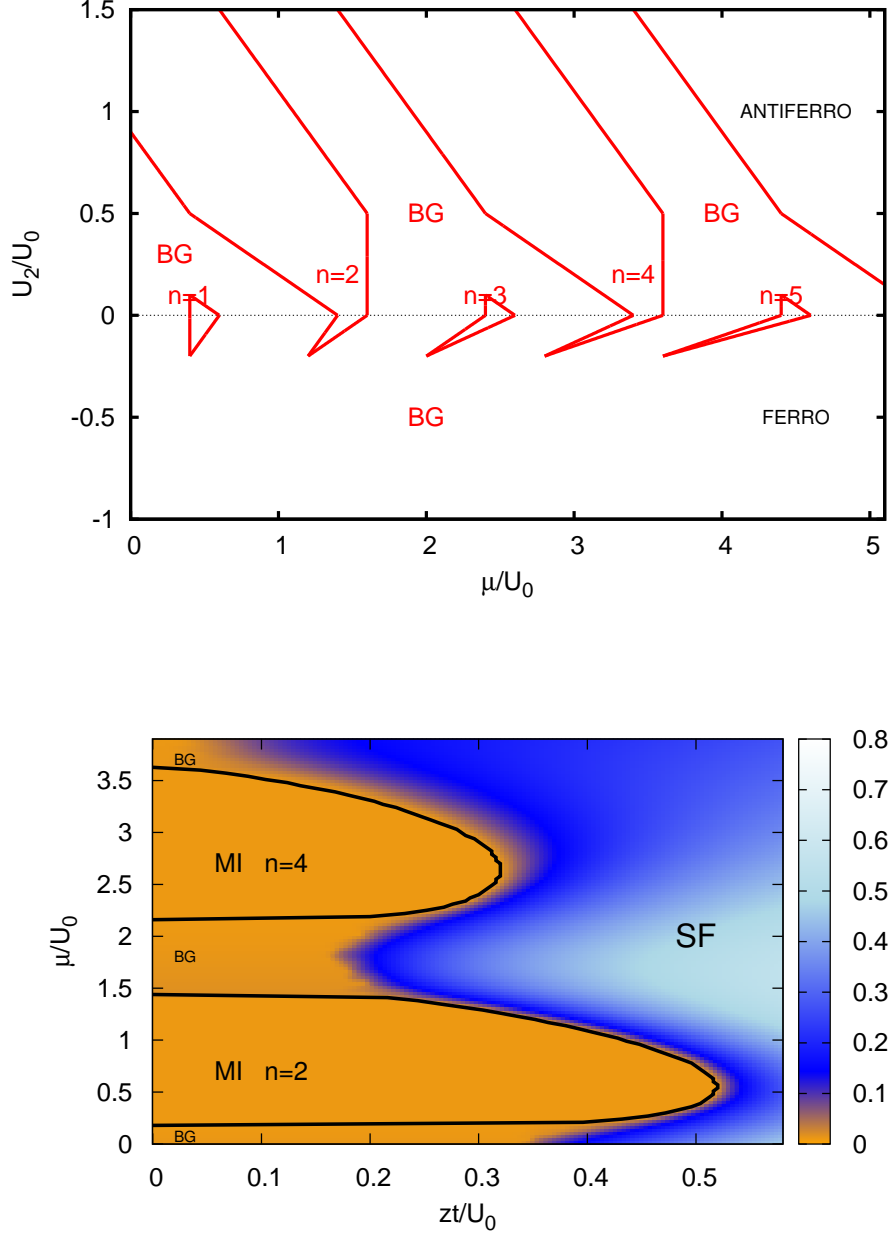


Fig. 2 (Color online) Top panel: phase diagram in the limit $t = 0$ and disorder in μ with $\Delta/U_0 = 0.4$. Bottom panel: condensate fraction with disorder in μ for $U_2/U_0 = 0.7$ and $\Delta/U_0 = 0.4$. The solid lines correspond to the boundaries of the MI lobes. The region outside the MI phase and with vanishing condensate fraction corresponds to the BG. In this case BG is formed by singlets.

the new scattering lengths become site-dependent $\alpha_s^j = \alpha_s + \varepsilon_j$. This represents a more realistic scenario than considering disorder in U_0 or U_2 alone.

To find the phase diagram in the atomic limit, we have to modify again the boundaries in (6-9) as we did in the previous section in the cases of disorder in U_0 and U_2 , remembering that, this time, both of them fluctuate at the same time. So, in the case of disorder in α_2 , one has to do the replacement $U_0 \rightarrow U_0 \mp 2\Delta$ and $U_2 \rightarrow U_2 \mp \Delta$ for $U_2/U_0 > 0$ and $U_2 \rightarrow U_2 \pm \Delta$ for $U_2/U_0 < 0$. The fluctuations occur, with amplitude $\tilde{\Delta} = 2\Delta \sqrt{(2\mu^0)^2 + (U_0 - 2U_2^0)^2 / (U_0 - 4\Delta^2)}$, along the direction (10) with $a = (U_2^0 + U_0)/\mu_0$ and $b = 0.5$

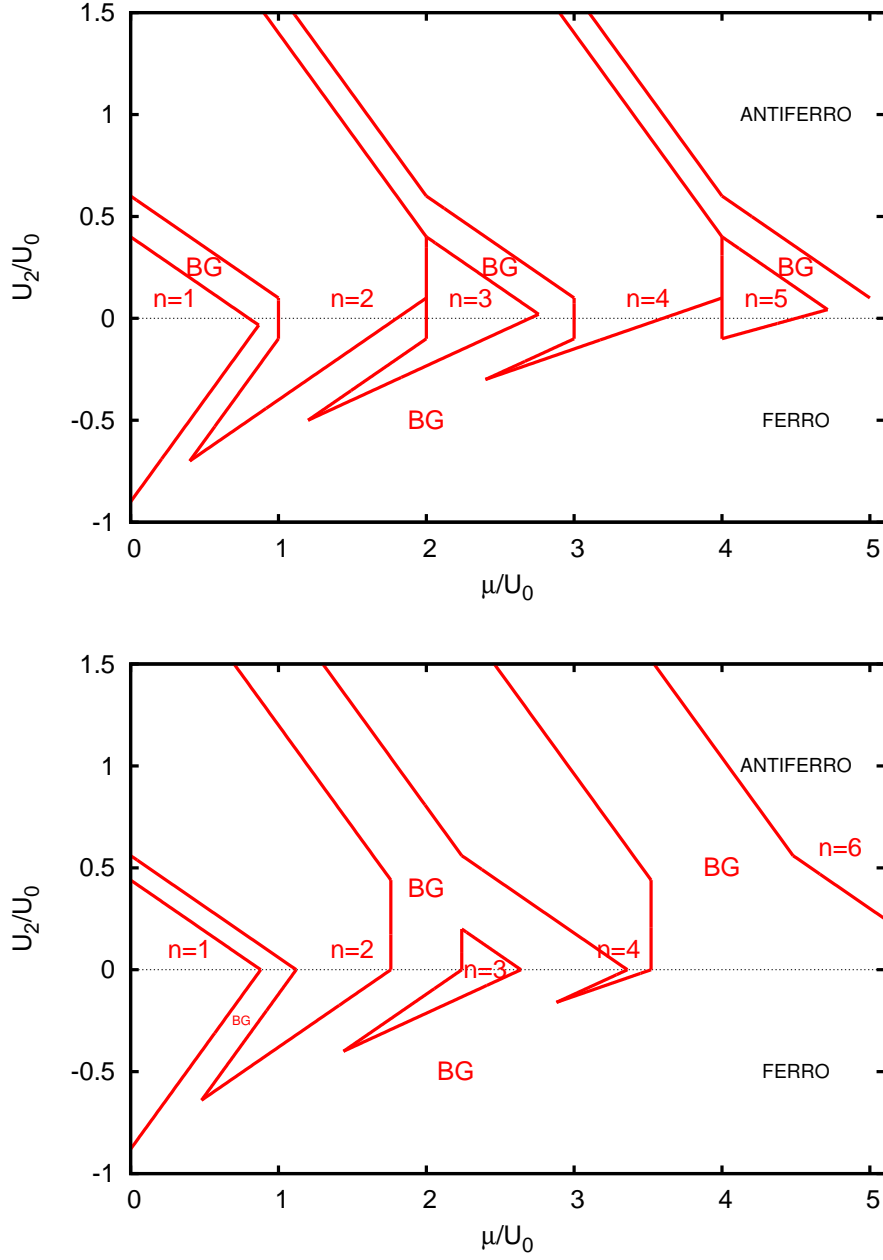


Fig. 3 Top panel: phase diagram in the limit $t = 0$ and disorder in U_2 with $\Delta/U_0 = 0.1$. Bottom panel: phase diagram in the limit $t = 0$ and disorder in U_0 with $\Delta/U_0 = 0.12$.

which is a family of straight lines passing through $(\mu/U_0 = 0, U_2/U_0 = 0.5)$. This means that the boundary between first and second lobe belongs to this family and no BG is expected between these two MI regions, as can be observed in both the atomic-limit (top panel) and complete phase (bottom panel) diagram in Fig. 4.

If the disorder is set in α_0 , substitutions in Eqs. (6-9) are $U_0 \rightarrow U_0 \mp \Delta$ and $U_2 \rightarrow U_2 \pm \Delta$ for $U_2/U_0 > 0$ and $U_s \rightarrow U_s \mp \Delta$ ($s = 0, 1$) for $U_2/U_0 < 0$. The direction of the fluctuations is given by $a = (U_2^0 + U_0)/\mu_0$ and $b = -1$ and amplitude $\tilde{\Delta} = 2\Delta \sqrt{(\mu^0)^2 + (U_0 + U_2^0)^2}/(U_0 - \Delta^2)$. In this case, all the boundaries in the ferromagnetic limits lie on fluctuation directions so no BG appears in the ferromagnetic regime as is shown in the top panel of Fig. 5. This result marks a distinction between the scalar case and the spinor one with ferro-

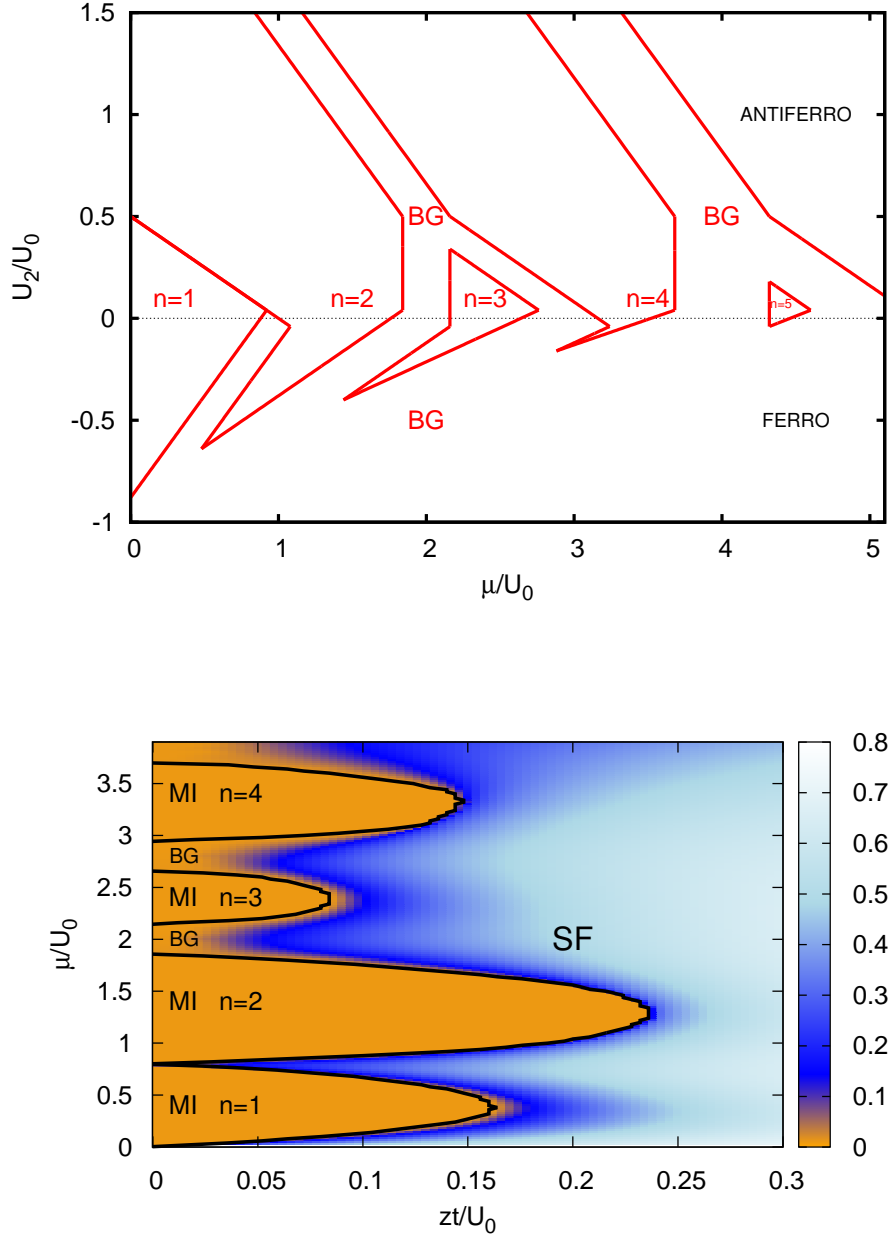


Fig. 4 (Color online) Disorder in α_2 with $\Delta/U_0 = 0.04$. Top panel: atomic limit. Bottom panel: finite hopping phase diagram with $U_2/U_0 = 0.1$.

magnetic spin correlations where disorder in the $s = 0$ scattering channel only is not enough to produce BG. The finite-hopping phase diagram for the antiferromagnetic regime where MI lobes are always surrounded by BG is shown in the lower panel of Fig.5.

5 Conclusions

We have analysed the spin-1 Bose Hubbard model with different types of diagonal disorder, focusing on the atomic limit to illustrate how Bose Glass phase emerges in between Mott lobes. In this limit, disorder mixes

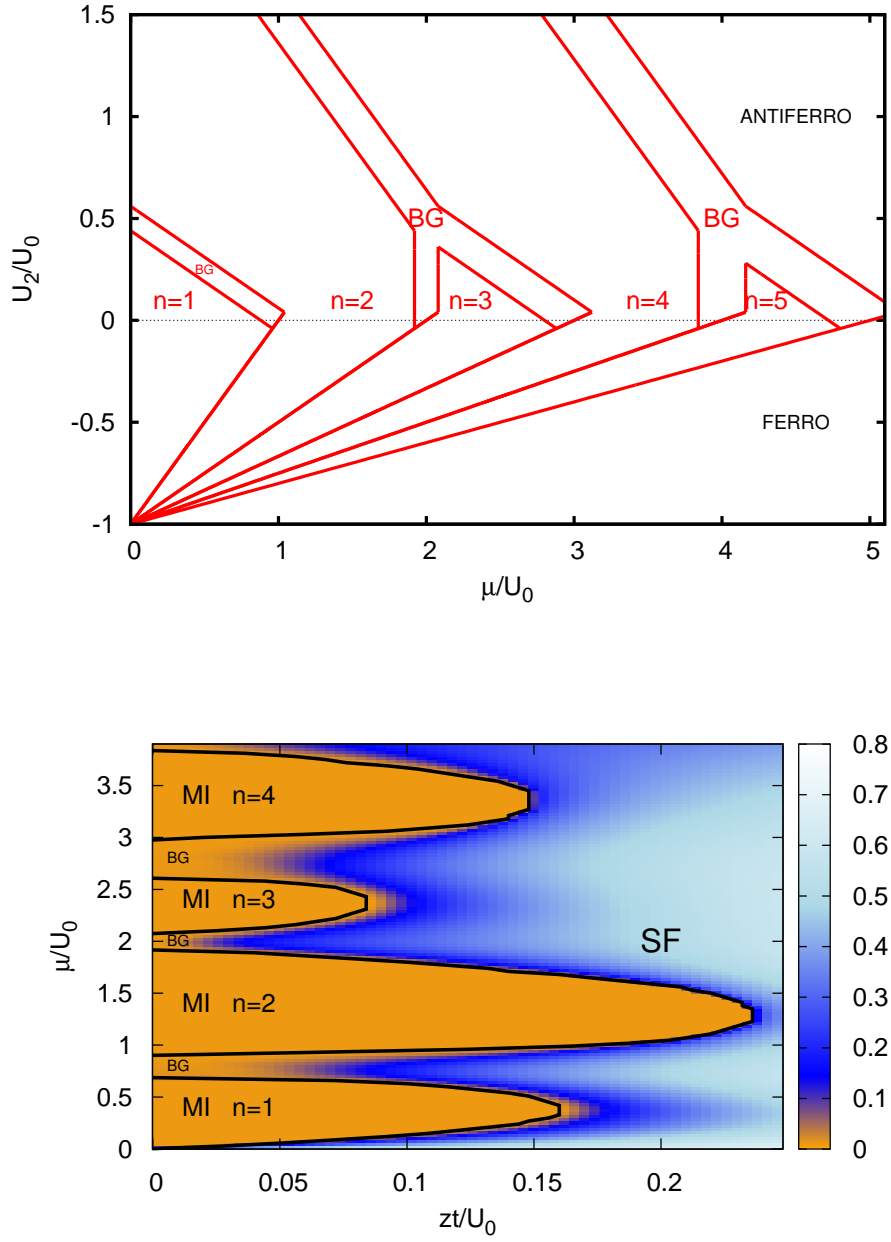


Fig. 5 (Color online) Disorder in α_0 with $\Delta/U_0 = 0.04$. Top panel: atomic limit. Bottom panel: finite hopping phase diagram with $U_2/U_0 = 0.1$.

MI phases with different occupation numbers, producing regions of BG between MI intervals. The study of the atomic limit gives useful information also about the finite hopping case, providing the structure of the phase diagram near the basis of the MI lobes. To illustrate the power of this approach, we have also shown in some cases the complete phase diagram, calculated by Gutzwiller approximation. We first analysed disorder, in either the chemical potential or the local interaction U_0 and U_2 , explaining how to construct the phase diagram in the atomic limit. Then, we used these results to study the more realistic case of disorder in one of the two scattering lengths a_0 or a_2 corresponding to different scattering channels. While in the scalar case BG always appears between MI regions, as soon as a small disorder is introduced, the spinor character can

stabilise the MI phase for some densities or spin interactions inhibiting the BG creation near its boundary. That happens in the case of disorder in U_2 between lobes with $n = 2m$ and $n = 2m + 1$, for disorder in a_0 in the ferromagnetic limit corresponding to $U_2/U_0 < 0$ as well as for disorder in a_2 between the first and second lobe. The creation of singlets in the even occupation MI enhances the stability of this phase, reducing the odd occupation MI lobes. As a consequence, the odd lobes are also less stable under the effect of disorder. In the extreme case in which odd lobes disappear also without disorder, the BG assumes a spin structure of singlet. As a future perspective, we would like to extend the approach we have illustrated in this paper to better enter into the spin properties of BG phases as well as the MI in the regimes where ferromagnetic and antiferromagnetic orders are mixed by disorder without destroying the MI phase. In this limit some new interesting phases could appear where the glassy character is not embedded in the density but in the spin degrees of freedom.

Acknowledgements We thank M. Lewenstein for useful discussions. Support from Polish Government (via research projects N202 079135 for 2008-2011 (MŁ) and N202 124736 for 2009-2012 (JZ)), Spanish Government (FIS2008:01236;02425, Consolider Ingenio 2010 (CDS2006-00019)) and Catalan Government (SGR2009:00347;00343) is acknowledged. J. Z. acknowledges hospitality from ICFO and partial support from the advanced ERC-grant QUAGATUA. M.Ł. acknowledges support from Jagiellonian University International Ph.D Studies in Physics of Complex Systems (Agreement no. MPD/2009/6) provided by Foundation for Polish Science and cofinanced by the European Regional Development Funds. S.P. is supported by the Spanish Ministry of Science and Innovation through the program Juan de la Cierva. Computer simulations were performed at ACK Cyfronet AGH as a part of the POIG PL-Grid project (M.Ł.).

References

1. A. Imambekov, M. Lukin and E. Demler, *Phys. Rev. A* **68**, 63602, (2003)
2. M.P.A. Fisher, P.B. Weichman, G Grinstein and D.S. Fisher, *Phys. Rev. B* **40**, 546, (1989)
3. S. Tsuchiya, S. Kurihara and T. Kimura, *Phys. Rev. A* **70**, 43628, (2004)
4. M. Rizzi, D. Rossini, G. De Chiara, S. Montangero and R. Fazio, *Phys. Rev. Lett.* **95**, 240404, (2005)
5. M. Lewenstein, A. Sanpera, V. Ahufinger, B. Damski, A. Sen and U. Sen, *Adv. Phys.* **56**, 243, (2007)
6. P. Horak, J.Y. Courtois and G. Grynberg, *Phys. Rev.* **58**, 3953, (1998)
7. D. Boiron et al., *Eur. Phys. J. D* **7**, 373, (1999)
8. R. Roth and K. Burnett, *Phys Rev A* **68**, 23604, (2003)
9. B. Damski, J. Zakrzewski, L. Santos, P. Zoller and M. Lewenstein, *Phys. Rev. Lett* **91**, 80403, (2003)
10. R.B. Diener, G.A. Georgakis, J. Zhong, M. Raizen and Q. Niu, *Phys. Rev. A.* **64**, 33416, (2001)
11. U. Gavish and Y. Castin, *Phys. Rev. Lett* **95**, 20401, (2005)
12. P. Massignan, Y. Castin, *Phys. Rev. A* **74**, 13616, (2006)
13. H. Gimpferlein, S. Wessel, J. Schmiedmayer and L. Santos, *Phys. Rev. Lett.* **95**, 170401, (2005)
14. C. Chin, R. Grimm, P. Julienne and E. Tiesinga, *Rev. Mod. Phys.* **82**, 1225, (2010)
15. M. Łącki, S. Paganelli, V. Ahufinger, A. Sanpera and J. Zakrzewski, *Phys. Rev. A* **83**, 013605, (2011)
16. T.L. Ho, *Phys. Rev. Lett.* **81**, 742, (1998)
17. T. Ohmi and K. Machida, *J. Phys. Soc. Jpn.* **67**, 1822, (1998)
18. C.K. Law, H. Pu and N.P. Bigelow, *Phys. Rev. Lett.* **81**, 5257, (1998)
19. D. Jaksch, C. Bruder, I. Cirac, C.W. Gardiner and P. Zoller, *Phys. Rev. Lett.* **81**, 3108, (1998)
20. M. Koashi and M. Ueda, *Phys. Rev. Lett.* **84**, 1066, (2000)
21. Y. Wu, *Phys. Rev. A* **54**, 4534, (1996)
22. E. Demler and F. Zhou, *Phys. Rev. Lett.* **88**, 163001, (2002)